

# LS-DYNA<sup>®</sup> Applications in Simulating Impact Tests of Nuclear Fuel Spacer Grids and Drop Tests of Fuel Shipping Packages

Wei Zhao, Zeses Karoutas, Paul Evans and Olin McRae  
Westinghouse Electric Company, LLC  
Columbia, SC 29250, USA

## Abstract

*Presented in the paper are two of our recent LS-DYNA applications in developing simulation models for: (1) impact tests of spacer grid – a key structural component of nuclear fuel, and (2) drop tests of shipping packages for fresh nuclear fuel, as described in the following, in that order.*

*Resistance of nuclear fuel structure to impact loads during postulated seismic and/or loss-of-coolant accident (LOCA) events needs to be demonstrated to show that no excessive fuel structural deformation would occur so that the three criteria are met: (i) fuel rod fragmentation does not occur, (ii) control rod insertion is ensured, and (iii) the core coolable geometry is maintained. The demonstration is accomplished through comparison of prediction through full core simulation with the strengths of the various structural components of the fuel. The impact tests of the spacer grids provide one such strength. As the impact test of the spacer grids requires significant lead time and effort, capability to simulate the spacer grid behavior under testing conditions is of great interest. More importantly, it provides a powerful tool for design.*

*To meet shipping package safety requirements for transporting fresh nuclear fuel assemblies, structural performance of the shipping package under hypothetical accident conditions must be evaluated and demonstrated to have adequate protection to the fuel assembly it transports. To efficiently evaluate design changes in the shipping package, a simplified finite element model for the shipping package and fuel assembly has been developed using LS-DYNA. The development and validation of the finite element model, along with a few design analysis examples to illustrate its usefulness are described.*

## 1. Simulating Impact Tests of Nuclear Fuel Spacer Grids

### 1.1 Introduction

Operating under harsh environmental and severe loading conditions inside nuclear reactors, fuel assembly's (FA) structural integrity must be maintained to insure safe and economic operation during normal working conditions. Furthermore, resistance of nuclear fuel structure to impact loads during postulated seismic and/or loss-of-coolant accident (LOCA) events must be demonstrated to show that no excessive fuel structural deformation would occur so that the three criteria are met: (i) fuel rod fragmentation does not occur, (ii) control rod insertion is ensured, and (iii) the core coolable geometry is maintained. The demonstration is accomplished through comparison of prediction through full core simulation with the strengths of the various structural components of the fuel. Figure 1(a) shows a typical pressure water reactor (PWR) fuel assembly, and its critical structural components, spacer grids, Figure 1(b). As a key element in demonstrating compliance of the criteria, impact tests of the spacer grids provide grid crush strength. As the impact test of the spacer grids requires significant lead time and effort, capability to simulate the spacer grid behavior under testing conditions is of great interest. More importantly, it provides a powerful tool for design, as fabrication of newly-designed spacer grids requires long lead time due to an iterative die design and testing process.

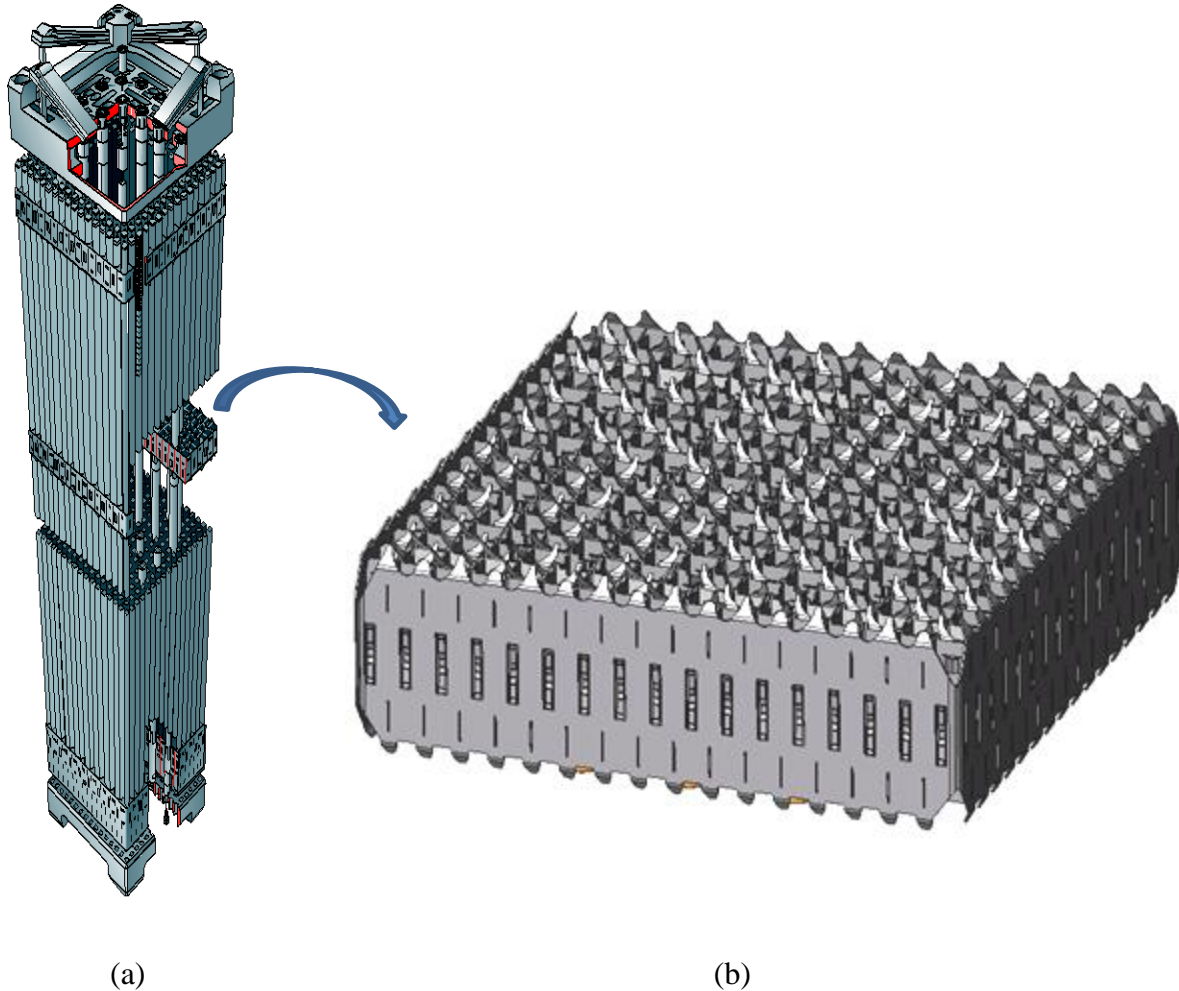


Fig. 1 (a) typical pressure water reactor fuel assembly, (b) typical spacer grid.

## 1.2 Grid LS-DYNA Model Development

The model development process involved the following key steps:

- Study of drawings
- Decide on important structural features to include, and those unimportant to omit
- Devise strategy for model development
- Strap model development for all straps.
- Grid model development using strap models
- Develop thimble sleeve models
- Add thimble sleeve models to the grid model
- Create simple weld joints at strap intersects of the grid model
- Develop cladding models
- Add cladding models to the grid model
- Develop weld nugget models
- Add nugget models to the grid model

Model testing at various stages was performed to establish, thus proceed on solid footings. The resulting model is shown in Figure 2.

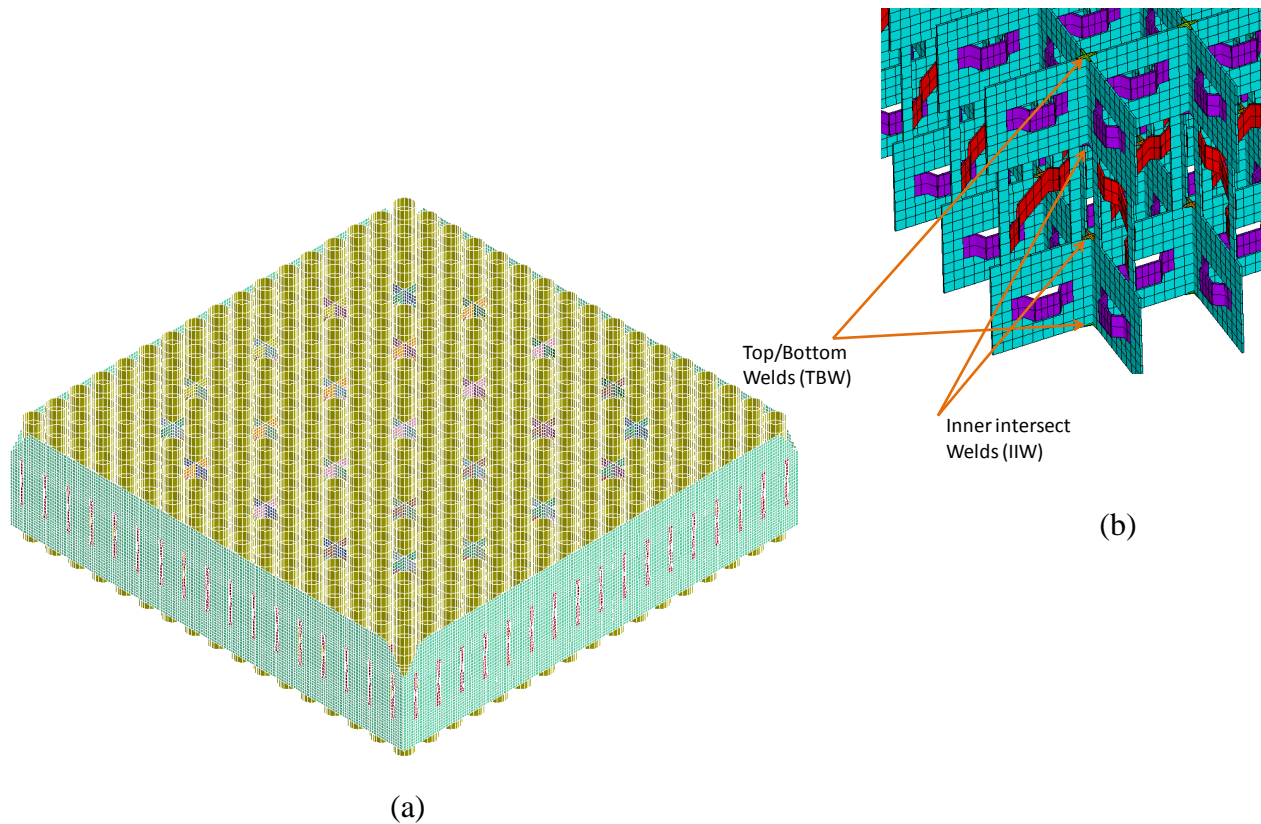


Fig.2 (a) Spacer grid model, (b) model cutout showing cell details.

### 1.3 Example Cases Analyzed

Various numerical simulations have been performed to check the model, and confirmed that the model behaves qualitatively reasonable based on experimental experiences, though the model is still pending to be tested against experimental data. Nevertheless, the model has been used to analyze a few cases of interest in design. Two examples are given below.

#### *Effect of inner strap thickness on grid crush strength*

To assess the effect of inner strap thickness on grid crush strength, three different inner strap thickness values were considered, corresponding to the minimum (0.017"), nominal (0.018"), and the maximum (0.0193") values according to allowable tolerances. In each case, all the inner straps assumed the same thickness. The grid was impacted by a 180 lbf hammer at an initial velocity of 30 in/s. Figure 3 shows isometric and top views of the deformed shape of the grid model. Figure 4 shows normalized grid crush strength vs. inner trap thickness for two cases: upper (red) curve for case without fuel rod cladding, while the lower (blue) curve for case with fuel rod cladding. The lower (blue) curve shows that, comparing with the nominal strap thickness, (1) 6% decrease from nominal thickness leads to a 20% decrease in crush strength, and (2) 7% increase from nominal thickness leads to 11% increase in crush strength. The upper (red) curve shows the same trend, but has a quite linear relationship with respect to the strap thickness, which is a reasonable behavior as adding fuel cladding sections introduces significant contact interactions between the cladding and the grid cell springs and dimples (the fuel rod support features), which is also a function of strap thickness.

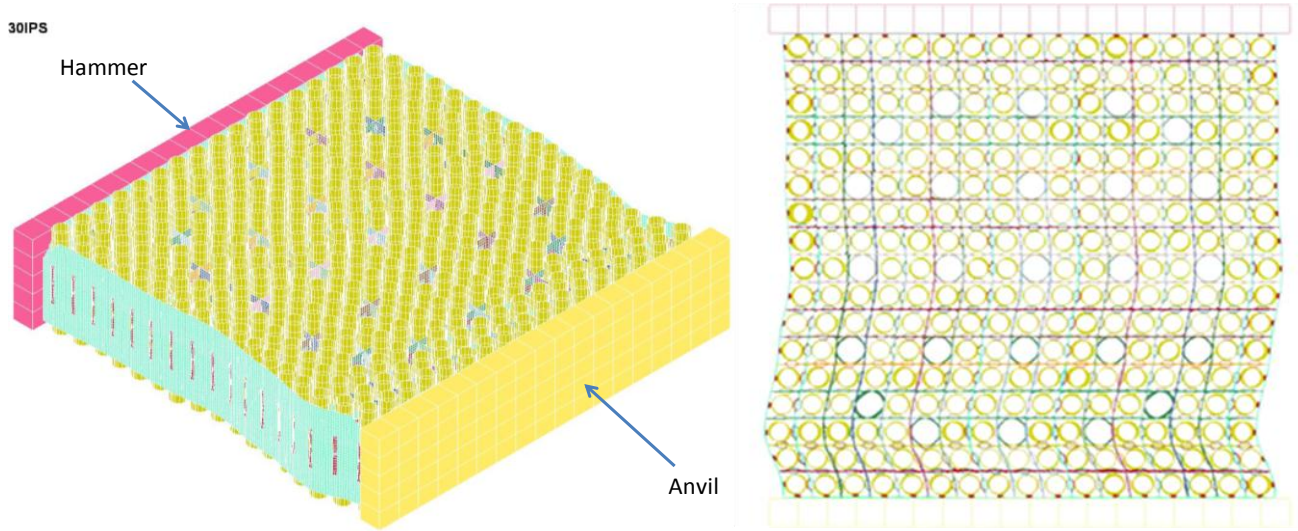


Fig. 3 Isometric and top views of deformed shape of the grid model.

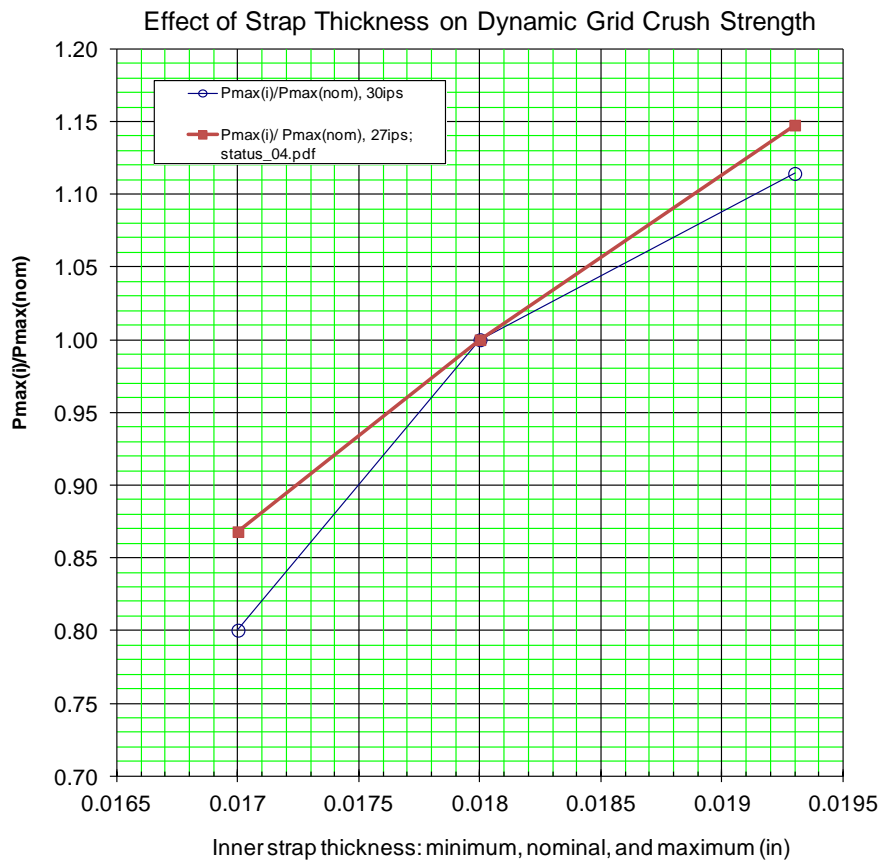


Fig.4 Normalized grid crush strength vs. inner trap thickness for two cases - upper (red) curve: without fuel rod cladding, lower (blue) curve: with fuel rod cladding.

*Effect of weld nugget shapes*

The effect of weld nugget shapes, i.e. pancake vs. carrot-shaped nuggets on crush strength. The pancake-shaped weld nuggets are centered around the intersect nodes and span to the adjacent in-plane nodes, as shown in Figure 5. Compared with the pancake-shaped weld nuggets, the carrot-shaped nuggets are also extended vertically to include the next node along the intersect edges next to the existing intersect weld.

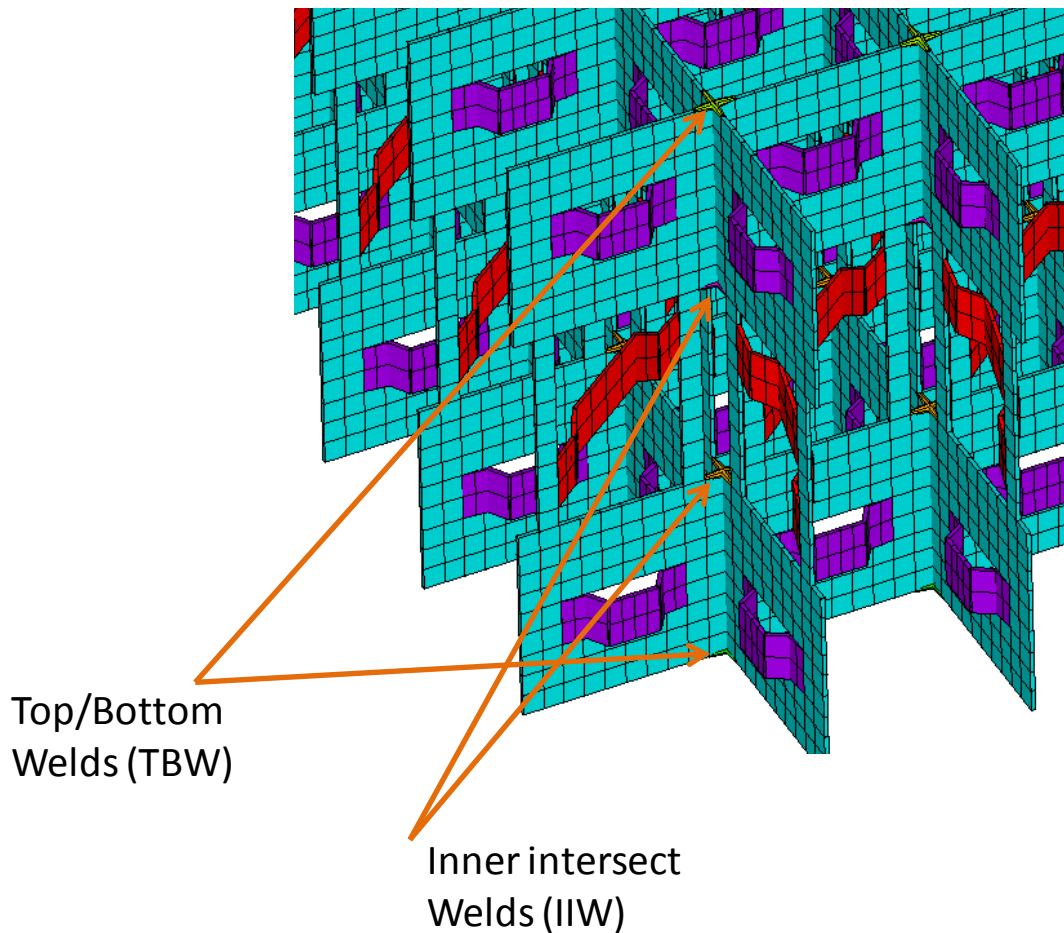


Fig.5 Weld nugget model and locations for the pancake-shaped weld.

The effect was evaluated for an impact condition of a 180 lbf hammer with an initial velocity of 30 in/s. The result shows a 42% increase in grid crush strength for the carrot-shaped nuggets over the pancake-shaped nuggets, a significant factor affecting crush strength. The top views of grid deformed shapes are shown in Figure 6(a) for grid model with the pancake-shaped nuggets, and in Figure 6(b) for grid model with the carrot-shaped nuggets.

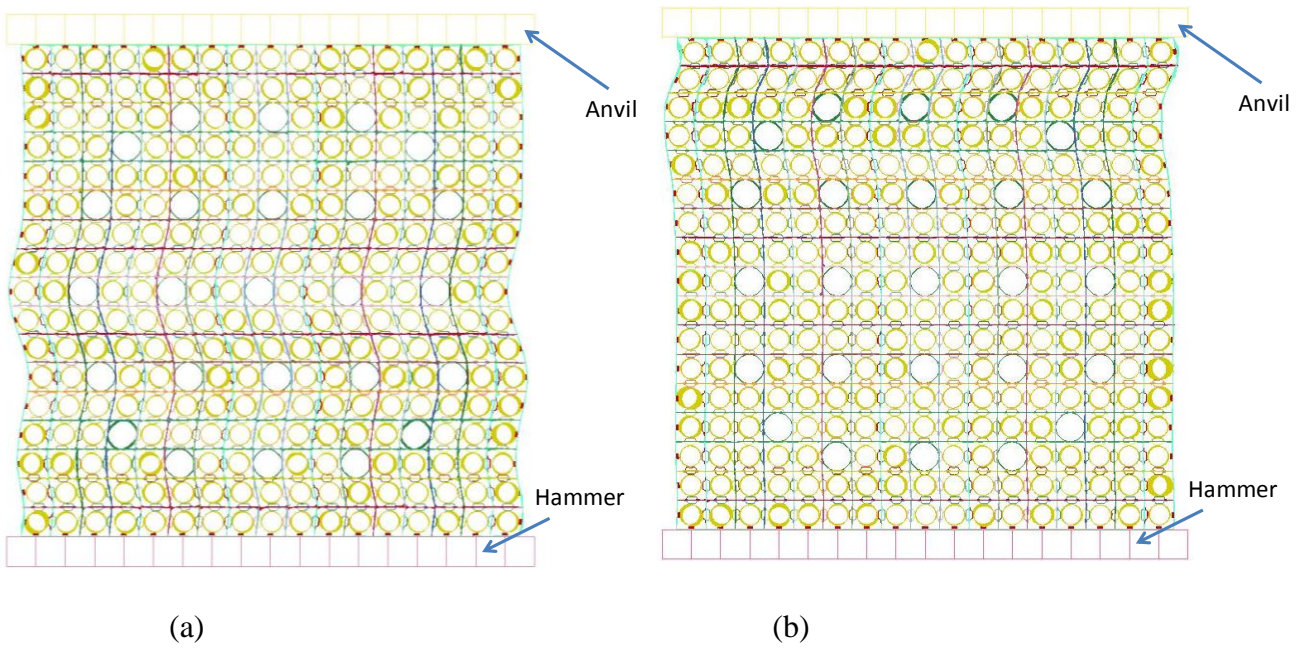


Fig. 6 Grid deformed shapes: (a) for pancake-shaped nuggets, (b) for carrot-shaped nuggets.

## 2. Simulating Drop Tests of Fuel Shipping Packages

### 2.1 Introduction

As dictated by the shipping package safety requirements for transporting fresh nuclear fuel assemblies [1, 2], structural performance of the shipping package under hypothetical accident conditions must be evaluated and demonstrated to have adequate protection to the fuel assembly it transports. Westinghouse has developed a new generation of shipping package, called Traveller<sup>TM</sup>, through detailed finite element modeling and simulation, complemented and validated with an extensive prototype testing program, which was partially documented in [3]. The primary structural features of the Traveller are shown as an exploded view in Figure 7.

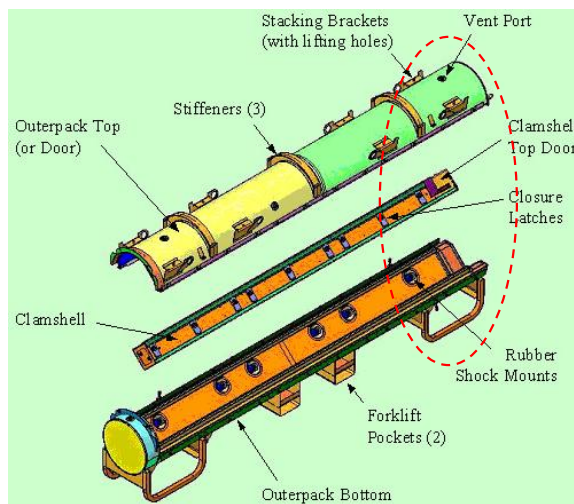


Fig.7 Major components of Traveller<sup>TM</sup>.

The fuel assembly is contained inside the Clamshell structure that is enclosed by the Outerpack. The Clamshell and the Outerpack are connected with rubber shock mounts so that shocks and vibrations during transportation are damped before reaching Clamshell and the fuel assembly. Relevant to the current effort in developing a simplified finite element model suitable for simulating the worst case scenario - vertical drop of the Traveller loaded with nuclear fuel onto its top end, the region of interest for detailed modeling is the area enclosed by the dashed curve in Figure 7. In order to efficiently evaluate design changes in the shipping package for adapting to different fuel assembly designs or different on-site fuel handling requirements, a simplified, but highly refined, finite element model for the shipping package and fuel assembly was developed using LS-DYNA. The simplified finite element model is used to simulate the worst case scenario in various hypothetical accident conditions. This worst case scenario has been identified as the vertical drop of a shipping package loaded with nuclear fuel onto its top end.

## 2.2 LS-DYNA Model Development

The structure of the shipping package consists of an Outerpack made from polyurethane foam encased in stainless steel sheets, and an inner housing (Clamshell) made from aluminum extrusions. To adequately represent the structural behavior in question, the finite element model contains all the details of the shipping package's end structure where the impact is to occur, and the fuel assembly's top nozzle with guide pins. The finite element model thus consists of three components: Outerpack, Clamshell and the fuel assembly's top nozzle, as described below.

### *Outerpack Model*

The Outerpack is made from polyurethane foam encased in stainless steel sheets. Figure 8(a) shows the FEA model for the foam region. Three different foam materials were used in the design, high density foam was used for the end impact limiter, low density foam was used for the pillow, and medium density foam was used for the Outerpack body. Figure 8(b) shows the FEA model for the entire Outerpack, where all foam materials are enclosed in stainless steel sheets plus additional stainless steel support plates. A cover plate was added to the end of the medium density foam, which contained the remaining mass of the Outerpack not included in the model. All the sheet metal components were modeled using 4-node shell elements (Belytschko-Tsay formulation with one-point reduced integration). The material property of the stainless steel was modeled using piecewise linear plasticity.

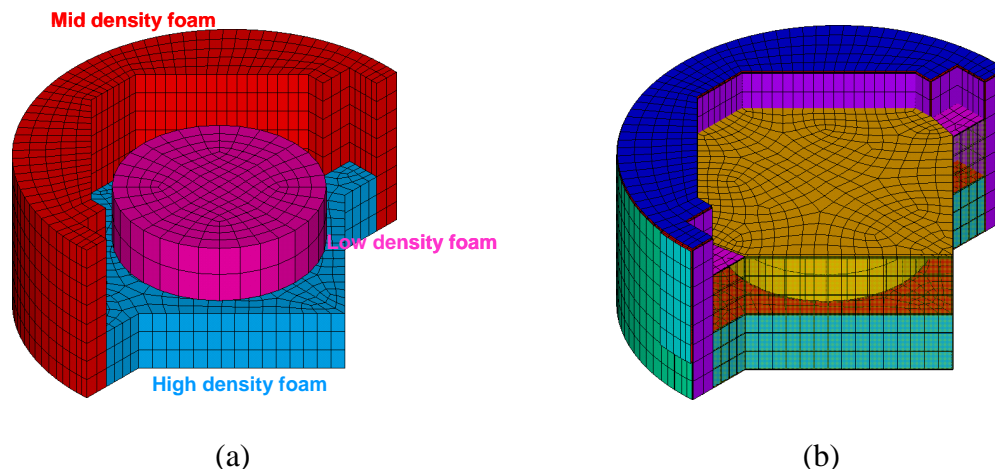


Fig.8 Outerpack FEA model, (a) foam material layout, (b) complete model.

All the foam components were modeled using 8-node brick elements (one-point reduced integration with viscous hourglass control). The material property of the foams was modeled using crushable foam.

#### Clamshell and Fuel Assembly Model

The Clamshell is made from aluminum extrusions, whose material behavior was modeled using plasticity with kinematic hardening. Stainless steel was used for the remaining components involved, including the restraining bar and studs, fuel assembly's top nozzle and guide pins. All components involved were modeled with brick elements mentioned above. Figure 9(a) shows the FEA model with two side walls of the Clamshell removed to reveal the inside. It is noted that the effect of remaining sections of the Clamshell and the fuel assembly were represented by condensed mass elements located respectively at the top surface nodes of the Clamshell and the fuel assembly, represented by the "\*" symbols. Figure 9(b) shows the entire model including the rigid ground, again with the two side walls of the Clamshell removed.

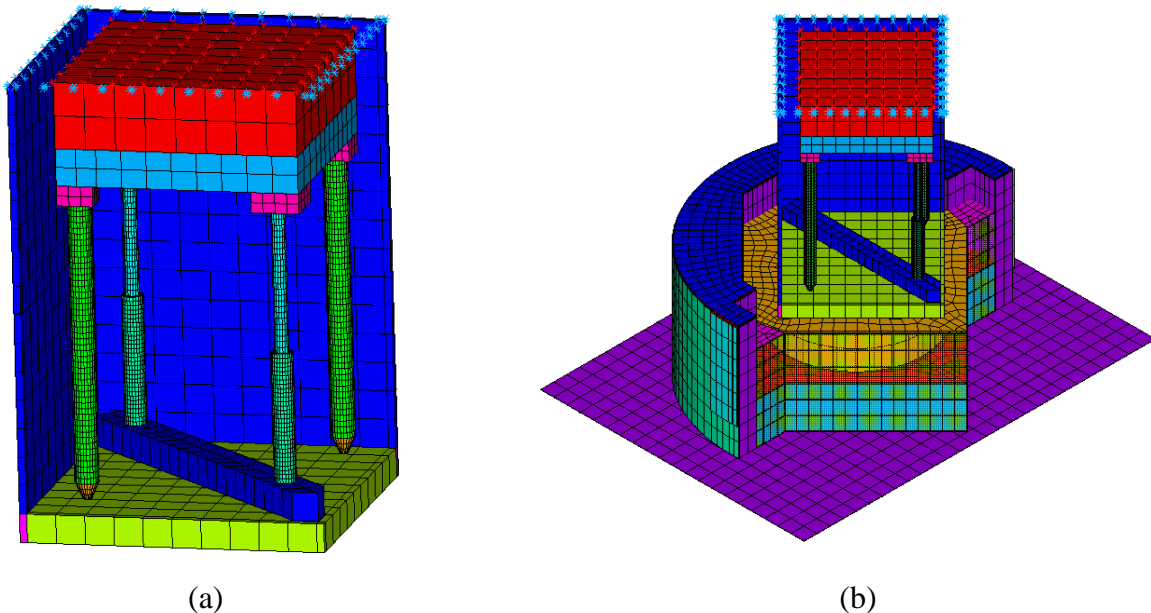


Fig.9 (a) Clamshell and fuel assembly model, (b) entire model.

### 2.3 Results and Discussions of Drop Test Simulation

First, the model was used to simulate a 10.15-meter drop test scenario to compare model results with an observation in the form of deformed shape from previously performed prototype drop test, as no quantitative test data is available for comparison in the model domain. Figure 10 shows such a comparison. The picture, Figure 10(b), was taken after 30-minutes pool-fire test that followed the drop test, thus the discoloration. The model did not contain the leaf springs, which were considered unimportant for the particular fuel design that has guide pins mounted on the top nozzle. The model deformed symmetrically as dictated by the symmetric model and drop conditions. The actual drop test on the other hand can never be perfectly symmetric, thus deformed in a non-symmetric manner. Nevertheless, one of the guide pins of the test article closely resembled the deformed shape of the model prediction. This close resemblance between the modal and the test represents a significant



improvement in the deformed shape prediction over that obtained in [3]. The other guide pin in the test article bent sideways and did not fold on itself, suggesting possible interaction between the pin and the leaf spring. The closer and improved prediction for the deformed shape over the validated model in [3] can be attributed to the highly refined FEA mesh affordable to the simplified model, and provided a degree of validation for the current simplified model.

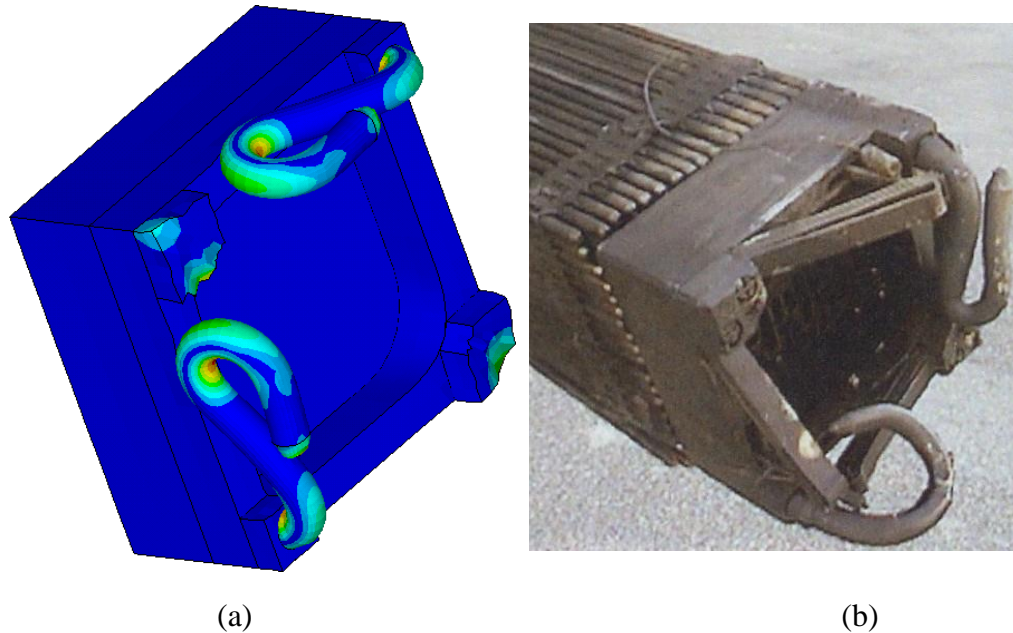


Fig.10 Comparison of deformed shapes for fuel assembly top nozzle between (a) model and (b) test.

To illustrate the impact event, a few stages of the deformation process are shown in Figure 11 for time instances of 5, 15 and 30 milliseconds (ms). For clarity, the rigid ground and the two side walls of Clamshell are not shown in Figure 11.

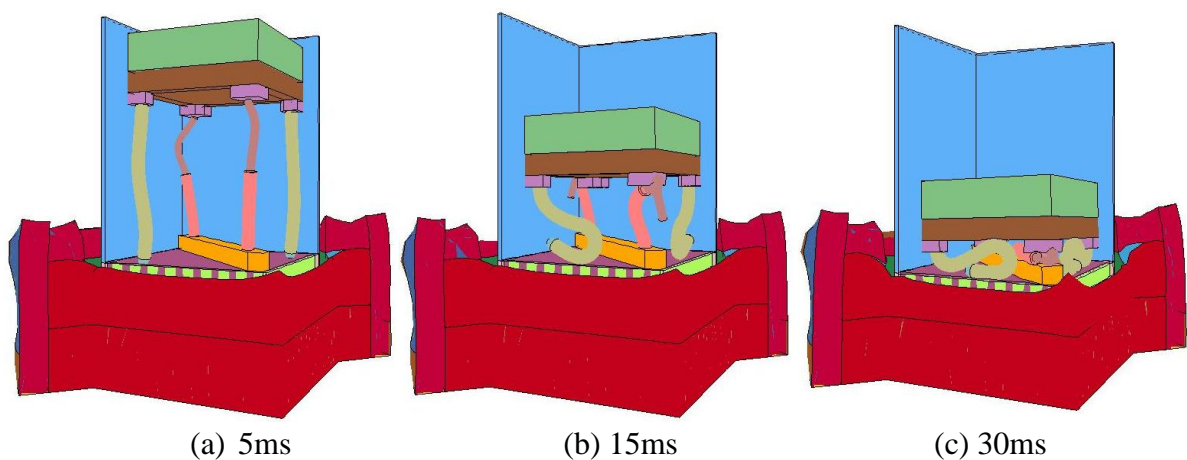


Fig.11 Deformation process at: (a) 5 ms, (b) 15 ms, and (c) 30 ms when kinetic energy reached zero.

Of primary interest to design are the impact-characterizing parameters, such as fuel assembly's acceleration, and impact limiters' (foam materials) cushioning effect. Figure 12 shows the deformation of the impact limiters and the fuel assembly's top nozzle acceleration versus time. It can be seen in Figure 12 that the impact limiters' deformation can be described in three stages. Stage I was an initial compression for a duration from 0 to ~5 ms, which caused by initial impact.

Stage II had a duration from ~5 to ~22 ms, during which no significant additional compression of the impact limiters was introduced. The existence of Stage II can be attributed to the buckling deformation process of the fuel assembly's guide pins and the restraining studs.

Stage III commenced at ~22 ms, when the deformation of the fuel assembly's guide pins and the restraining studs reached maximum, and significant further compression of the impact limiters occurred. The state of the maximum deformation for the guide pins and the restraining studs can be seen in Figure 11(c).

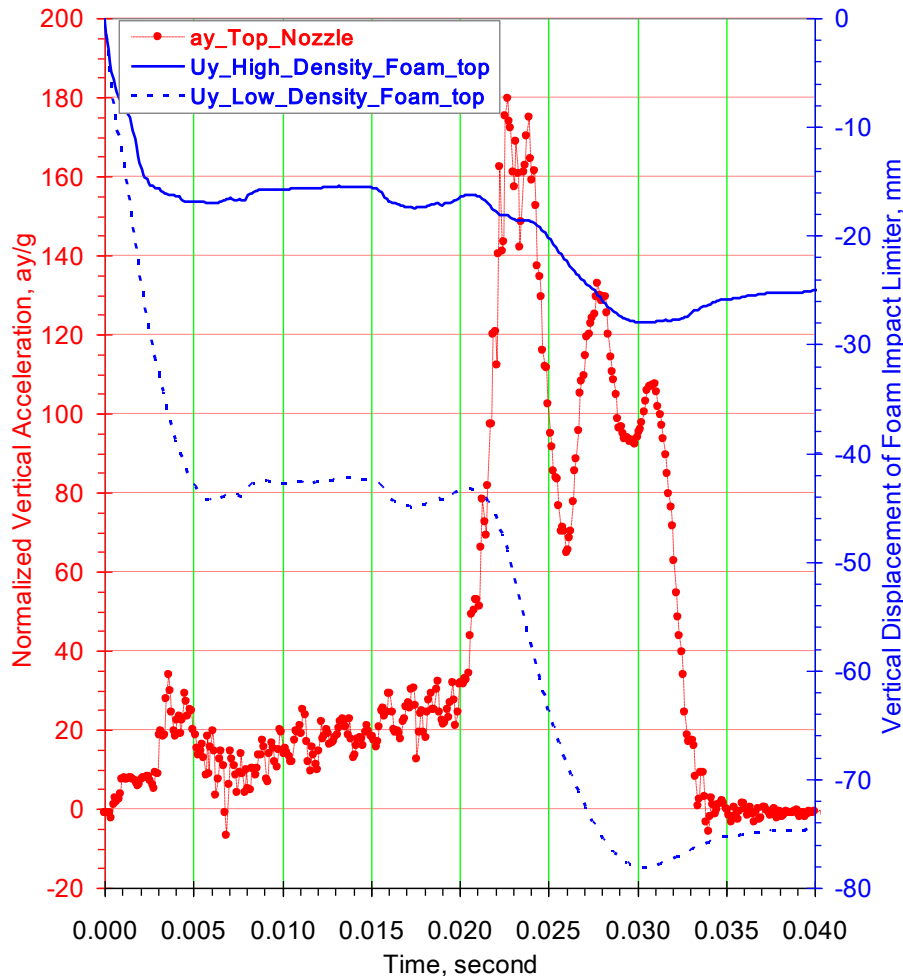


Fig. 12 Deformation of impact limiters and acceleration of fuel assembly's top nozzle: 10.15m drop.

The acceleration behavior for the fuel assembly's top nozzle can be well understood based on the above description of the impact limiters deformation process. The acceleration reached maximum when the deformation of the fuel assembly's guide pins and the restraining studs

reached maximum (flattened out). The acceleration thereafter varied largely according to the combined compression incremental behaviors of the two impact limiters with different foam densities.

#### *An Example – Effect of Reduced Fuel Assembly Weight*

The example considers the same drop height of 10.15m for a reduced fuel assembly weight to ~75% of the case shown in Figure 12 which represents our heaviest fuel assembly. The results for this lighter fuel are designated with suffix “\_rm75”. Figure 13 shows the results for the case of the reduced fuel weight.

In comparison with Figure 12, it is noted that the impact limiters were compressed less for the lighter fuel, as expected. Contrary to the intuition, however, the maximum acceleration for the fuel assembly’s top nozzle increased slightly. This was attributed to the reduced cushioning effect resulting from the reduced deformation of the impact limiters.

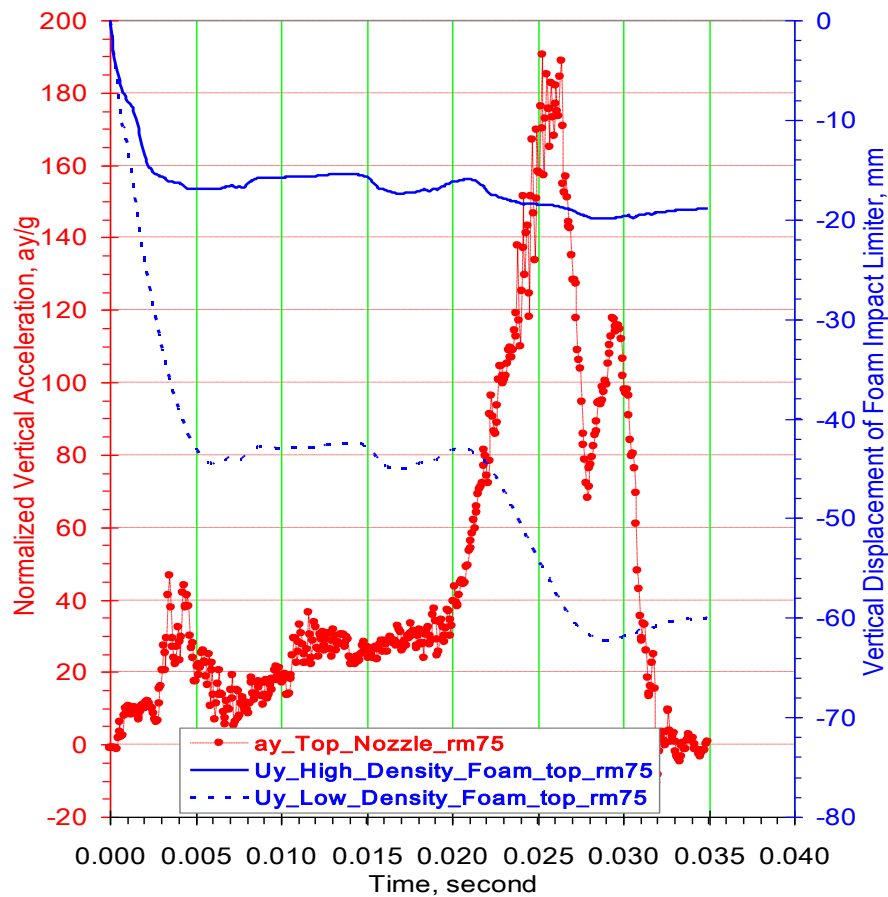


Fig. 13: Deformation of impact limiters and acceleration of fuel assembly’s top nozzle: 10.15m drop, reduced fuel weight.

In comparison with Figure 12, it is noted that the impact limiters were compressed less for the lighter fuel, as expected. Contrary to the intuition, however, the maximum acceleration for the fuel assembly’s top nozzle increased slightly. This was attributed to the reduced cushioning effect resulting from the reduced deformation of the impact limiters. This observation is revealing in that the heavier fuel’s behavior is not necessarily bound the

behavior for the lighter fuel in terms of impact severity, which also depends on the crush behavior of the impact limiters.

### **Summary**

It is shown that LS-DYNA<sup>®</sup> applications in simulating impact tests of nuclear fuel spacer grids and drop tests of fuel shipping packages provide insights and understanding of complicated processes and behaviors that can guide analysis and design, and shorten the design cycle.

### **References**

- 1 Title 10, Code of Federal Regulations for the Packaging and Transport of Radioactive Material, Part 71.73.
- 2 "IAEA Safety Standard Series Number ST-1," Section VII, "Regulations for the Safe Transport of Radioactive Material."
- 3 Staples, J.F., Pitzer, M., and DuBois, P.A., "Development of Shipping Package Drop Analysis Capability at Westinghouse," 8th International LS-DYNA Users Conference, Detroit, 2004.